

# Study on the ability of the three-dose-volume-histogram-gamma (3DVH- $\gamma$ ) analysis and bio-mathematical model in detecting dose changes caused by dose-calculation-grid-size (DCGS)

**Han Bai**

Yunnan Cancer Hospital <https://orcid.org/0000-0003-3593-1262>

**Sijin Zhu**

Radiation Oncology Centres

**Xingrao Wu** (✉ [916133705@qq.com](mailto:916133705@qq.com))

Yunnan Cancer Hospital

**Xuhong Liu**

Radiation Oncology Centre

**Feihu Chen**

Radiation Oncology Centres

**Jiawen Yan**

Radiation Oncology Centres

---

## Research

**Keywords:** 3DVH- $\gamma$  analysis, bio-mathematical model, dose calculation grid size (DCGS), dose change

**Posted Date:** May 25th, 2020

**DOI:** <https://doi.org/10.21203/rs.3.rs-17543/v2>

**License:**  This work is licensed under a Creative Commons Attribution 4.0 International License.

[Read Full License](#)

---

**Version of Record:** A version of this preprint was published on July 6th, 2020. See the published version at <https://doi.org/10.1186/s13014-020-01603-6>.

# Abstract

Objective : To explore the efficacy and sensitivity of 3DVH- $\gamma$  analysis and bio-mathematical model for cervical cancer in detecting dose changes caused by dose-calculation-grid-size(DCGS).

Methods 17 patients' plans for cervical cancer were enrolled Pinnacle TPS VMAT, and the DCGS was changed from 2.0mm to 5.0mm to calculate the planned dose respectively. The dose distribution calculated by DCGS = 2.0mm as the "reference" data set (RDS), the dose distribution calculated by the rest DCGS as the "measurement" data set (MDS), the 3DVH- $\gamma$  passing rates and the (N)TCPs of the all structures under different DCGS were obtained, and then analyze the ability of 3DVH- $\gamma$  analysis and (N)TCP model in detecting dose changes and what factors affect this ability.

Results: The effect of DCGS on planned dose was obvious. When the  $\gamma$ -standard was 1.0mm, 1.0% and 10.0%, the difference of the results of the DCGS on dose-effect could be detected by 3DVH- $\gamma$  analysis ( $p < 0.05$ ). With the decline of the standard, 3DVH- $\gamma$  analysis' ability to detect this difference shows weaker. When the standard was 1.0mm, 3.0% and 10.0%, the  $p$  value of  $>0.05$  accounted for the majority. With DCGS=2.0mm being RDS,  $\Delta\gamma$ -passing-rate presented the same trend with  $\Delta(N)TCPs$  of all structures except for the femurs only when the 1.0mm, 1.0% and 10.0% standards were adopted for the 3DVH- $\gamma$  analysis.

Conclusions: The 3DVH- $\gamma$  analysis and bio-mathematical model can be used to analyze the effect of DCGS on the planned dose. For comparison, the former's detection ability has a lot to do with the designed standard, and the latter's capability is related to the parameters and calculated accuracy intrinsically.

## Introduction

The dose calculation grid size (DCGS) is a basic parameter setting in the design of the plan. Usually, a commercial treatment planning system (TPS) will provide various DCGS within a certain range for designers to choose for different needs. For example, the commercial Pinnacle TPS provides DCGS ranging from 1.0mm to 10.0mm, and the default DCGS is 4.0mm. Larger DCGS is commonly adopted for calculation in cases with larger target volumes and organ-at-risk (OAR) volumes for better calculation efficiency. However, a smaller DCGS should be chosen for dose calculation in radiotherapy for head and neck tumors to obtain precise doses of small-volume OARs including lens, optic nerve and pituitary, etc., especially important for OARs with strict maximum dose limit [1,2].

The difference in doses caused by different grid sizes may affect the evaluation of the quality of physical solutions, although the DCGS can not cause the actual absorbed dose when the accelerator's parameters are certain. (This is why the planned dose values and (N)TCP values calculated under different DCGS are all called "calculated" values in the following sections). Therefore, it is a crucial task to understand the effect of DCGS on the physical and biological doses in radiotherapy for cervical cancer (CC).  $\gamma$  analysis is currently the most common and generally accepted method for quantitatively assessing the difference

between the two dose-distributions (DDs)[3,4]. It detects the difference between the two DDs by a designed  $\gamma$  standard (e.g. 3.0mm, 3.0%, 10%) and it will provide a report on passing rate[5,6]. The standard of 3.0mm, 3.0% and 10% is the most widely used, in which 3.0mm refers to the consistency of distance, 3.0% refers to the maximum allowable dose difference, and 10% is the threshold and when the dose is less than 10% of the reference dose, which does not participate in Gamma analysis. Selecting 10% is widely recommended[7,8]. In intensity modulated radiation therapy (IMRT),  $\gamma$  analysis is usually used to analyze the difference between the TPS-outputted and the actually measured dose distribution to evaluate the degree of dose deviation caused by various reasons during the execution of the plan, further to determine whether a plan is to execute based on the evaluation. However, previous studies have shown that different dose QA systems have different abilities to detect errors based on the dose distribution output by TPS. Hussein et al.[9] enrolled pelvis and head & neck IMRT and RapidArc™ plans, and compared the differences in the detecting dose error of five commercial products: PTW Verisoft, Delta4 software, SNC Patient, Varian Portal Dosimetry and IBA OmniPro. The results showed that for the same pass-rate criteria, different devices and software combinations exhibited varying levels of agreement with the predicted  $\gamma$  analysis. On the other hand, different gamma analysis standards will get different passing rates. Research by Heilemann et al.[10] showed that the 3.0mm, 3.0%, and 10.0% standards were not sufficient to detect the deviation caused by the MLC position uncertainty, and this standard, at least, has to be 2.0mm, 2.0%, 10.0%.

The focus on the variation of planned dose (PD) is due to the fact that it could cause changes in the biological effects. Specifically, in the clinical practice of radiotherapy, the alteration in physical dose will bring about changes in tumor control probability (TCP) and normal tissue complication probability (NTCP). Therefore, the current project, under the condition of DCGS changes, used the dose distribution calculated by DCGS=2.0mm as the reference data set (RDS) to explore the efficacy and sensitivity of the 3DVH- $\gamma$  analysis and the bio-mathematical model on dose change detection by analyzing the 3DVH- $\gamma$  passing rates of all structures and the relationship between  $\gamma$  passing rate and (N)TCP.

## Materials And Methods

### 1.1 Patient materials

A retrospective study was performed on the physical plan of 17 patients with CC who were treated in the Department of Radiation Therapy of our hospital from December 2017 to November 2018. And the 17 patients' plans were initially designed and evaluated with DCGS=4.0mm. The patient's PGTV volume was 20.0-395.0 cm<sup>3</sup>, and the PTV volume was 880.0-2587.0 cm<sup>3</sup>. The average volumes of the two target volume were 128.9±110.2cm<sup>3</sup>, 1752.9±460.1cm<sup>3</sup>, respectively. The rectum's mean volume was 59.3±25.4cm<sup>3</sup>, and the bladder's was 257.5±165.6cm<sup>3</sup>, and the L-femur's and R-femur's were 107.2±19.1cm<sup>3</sup>, 108.2±19.6cm<sup>3</sup>. These patients were in a supine position with both hands surrounding his head, and the patient was fixed with a thermoplastic mesh. The Siemens Somatom Sensation Open 24 CT (Siemens Co., Munich, Germany) was used as the data acquisition system. The range of scanning

was from the head of the diaphragm to lower 1.0cm of the bottom pubic symphysis. And the CT data of each patient was reconstructed with a 3.0 mm layer thickness, was transmitted to Pinnacle TPS 9.10.

## 1.2 Design of VMAT radiotherapy plan

17 patients were treated with a Versa HD linear accelerator (Elekta Medical Systems Co., Stockholm, Sweden) of 6 MV photon beams. The volumetric modulated arc therapy (VMAT) plan of a 360° full bow with 2 arcs was designed for every patient based on Smart Arc inverse optimization. The objective functions were shown in Table 1. The doses were calculated with the Collapsed Cone Convolution (CCC) algorithm. The CCC dose engine determines dose deposition by a three-dimensional convolution/superposition of the Total Energy Released per unit Mass (TERMA) with a dose spread function. The TERMA is determined by projection of the beam energy fluence through the patient CT volume. The effects of changes in tissue composition on dose distribution are approximated by scaling the dose spread function by the radiological distance to account for the presence of heterogeneities with respect to scattered radiation. The superposition of the calculated dose distribution from all TERMA volumes determines the final 3D dose distribution in patient [11]. The planning prescription setting was as follows: the planning target volume (PTV) prescription being 45.0-50.0Gy / 25F, and the planning volume of the gross tumor (PGTV) prescription being 60.0-62.5Gy / 25F.

All VMAT physical schemes were designed with Pinnacle TPS (version 9.10). When the default value was DCGS = 4.0mm, the planners optimized and adjusted the treatment plans for CC patients based on their own previous experience. After all the indicators of the plans met the clinical requirements, changed the DCGS (from 2.0mm to 5.0mm) and recalculated dose in the target volumes and OARs.

## 1.3 3DVH standard and passing rate

After the emergence of IMRT technology, verification of radiation dose before the implementation of treatment has become a very important part of the radiotherapy process. Dose verification can be divided into point dosimetry verification, plane dosimetry verification and gel dosimetry verification. The point dosimetry verification and Gel dosimetry verification [12,13] have not been widely accepted because of various reasons, and the plane dosimetry verification has become a popular method. The commercially available PTW-ARRAYs [14] and IAB-ARRAYs [15] are the most popular tools for plane dose verification. These ARRAYs only respond correctly to beams perpendicular to their matrix plane, and it is necessary to combine the scattered beams into one direction when using these ARRAYs. This feature makes these ARRAYs less suitable for dose verification of VMAT with rotating beams. So, Delta 4, ArcCheck and Octavius 4D for dose verification of VMAT are more common in daily work [16-18].

Although the tools advanced, there has been no fundamental change in analytical methods. The  $\gamma$  analysis has been used throughout IMRT dose verification. The commonly recommended  $\gamma$  analysis standards are 3.0mm, 3.0%, and 10% threshold [7,8], but studies have shown that, depending on the technology and the disease, we should adopt stricter standards or other supplement analysis to analyze errors [19,20].

The 3DVH-gamma analysis is also a standard gamma-analysis. The 3DVH-gamma-analysis is that during the dose of reconstruction before the analysis of gamma-analysis, the software will be used the planned dosed Perturbation (PDP) algorithm corresponding the hardware. For example, if the hardware is ArcCHECK, the corresponding algorithm is ArcCHECK-planned-dosed- perturbation (AC-PDP). AC-PDP is the engine behind 3DVH when used in conjunction with ArcCHECK 4D measured dose to generate quality assurance (QA) metrics based on patient dose and DVH. At the core of AC-PDP is true 4D Measurement Guided Dosed Reconstruction (MGDR), which generates a high-density, High-resolution 3D dose estimate using the ArcCHECK dose movie data which has time resolved to 50 msec and an integrated virtual inclinometer (VI) [21].

This article was to investigate errors among planned dose caused by DCGS with dose distribution calculated by DCGS=2.0mm as RDS and the dose distribution calculated by DCGS=3.0mm, 4.0mm, 5.0mm as MDS, respectively. And we thought the location uncertainty was scarcely influential element under the situation. Therefore, when setting the  $\gamma$  analysis standard, we setted the following 3 standards: 1.0mm, 1.0%, 10% threshold; 1.0mm, 2.0%, 10% threshold; 1.0mm, 3.0% , 10% threshold.

#### 1.4 TCP and NTCP calculation

The link between physical dose (change) and biological effect (change) has always been our focus. Changes in DCGS will certainly bring about changes in the physical dose, as well as the biological effects. It is well known that changes in biological effects have more direct clinical significance, so this study ignored the physical dose and directly calculated the changes in biological effects caused by changes in DCGS by using biological model.

Some biologically related models for plan optimization and/or evaluation have been introduced into treatment planning tools for clinical use. A variety of dose- response models with a series of organ-specific model parameters were reported in the literatures, and were widely accepted as follows[22,23]:

[Please see the supplementary files section to view the equations.]

(2.1)

(2.2)

(2.3)

(2.4)

Where,  $a$  is an organ-specific constant, and its corresponding value is in the literatures[24,25].  $v_i$  is the fractional volume of the organ receiving  $D_i$ .  $m$  and  $n$  are unique organ-specific constants[24,25].  $TD_{50}$  is an uniform dose that is absorbed dose at a 50% complication probability, and  $TCD_{50}$  is an uniform dose that is absorbed dose at a 50% control probability.

## 1.5 Statistical analysis

Origin 8.0 was used for drawing and SPSS 20.0 was used for statistical analysis. *Paired t test* was used for statistical analysis, and  $p > 0.05$  indicates no significant difference, and  $0.01 < p < 0.05$  indicates significant difference, and  $p < 0.01$  indicates very significant difference.

## Results

### 2.1 (N)TCP and absolute dose (AD) changes with DCGS

DCGS's change indicated the change of "collection-dose-unit". Key dose points on DVH of each structure with DCGS's change were counted and analysed. As we all know, for target, minimum dose (MinD), maximum dose (MaxD) and mean dose (MeanD) were important for efficacy [26]. And for organ-at-risk, MeanD was important for toxicity [27]. So, we counted on PGTV's MinD, MaxD and MeanD, and PTV's MinD and MeanD (because PGTV is included in PTV, the maximum dose in PTV is located in PGTV), and MeanD of Bladder, Rectum and Femurs (shown in Fig 1- Fig 4).

The 68 differential DVHs of 17 patients' radiotherapy plans ( $17 \times 4 = 68$ ) were exported as .txt data files. The data in the .txt file were read by MATLAB program and put into formulas (1) and (2.4) to calculate the EUD of each OAR and each target. Then TCP and NTCP were calculated using the formulas (1) and (2.1). Figures drawn by Origin 8.0 software were shown in Fig 5 and Fig 6. As shown in the figures, the influence of DCGS on the calculated value of (N) TCP was obvious, and the calculated value of (N) TCP decreased with the increase of DCGS.

**Fig 1.** Display of MinD, MaxD and MeanD of PGTV change caused by DCGS

**Fig 2.** Display of MinD and MeanD of PTV change caused by DCGS

**Fig 3.** Display of MeanDs of Rectum and Bladder change caused by DCGS

**Fig 4.** Display of MeanDs of R-Femur and L-Femur change caused by DCGS

**Fig 5.** Display of TCP change caused by DCGS

**Fig 6.** Display of NTCP change caused by DCGS

### 2.2 *p*-value analysis

The change of DCGS would bring about the change of each structure's absorption dose. In order to quantify the DC, we selected  $\gamma$  analysis to analyze the difference between the dose corresponding to DCGS=2.0mm acting as RDS and the dose corresponding to DCGS=3.0mm, 4.0mm, 5.0mm acting as MDS, respectively.

In order to reflect the statistical significance of the dose difference caused by different DCGS, we grouped and named the results of  $\gamma$  analysis, as shown in Table 2. For example, when the  $\gamma$  analysis standard setting was 1.0mm, 1.0%, 10.0% and the dose distributions of DCGS=3.0mm and DCGS=2.0mm were compared, the results were grouped as Aa. And the paired  $t$ -test results of each structure were shown in Fig. 7. They-standard had a significant impact on the  $\gamma$ -analysis' sensitivity. When the  $\gamma$ -standard was 1.0mm, 1.0% and 10.0%, the difference of the results of the DCGS on dose-effect could be detected by 3DVH- $\gamma$  analysis ( $p < 0.05$ ). With the decline of the standard, 3DVH- $\gamma$  analysis' ability to detect this difference was also declining. When the standard was 1.0mm, 3.0% and 10.0%, the  $p$  value of  $> 0.05$  accounted for the majority. It was a high probability event that the dose difference between DCGS=0.5mm and DCGS=3.0mm (or the other two DCGSs) could not be detected by this analysis.

**Fig 7.** The map of every structure's paired  $t$  test under varied  $\gamma$  analysis standard.

### 2.3 Correlation of $\Delta$ (N)TCP and $\Delta$ $\gamma$

The (N)TCPs' and  $\gamma$  values both changed with DCGS. To explore whether there was a certain correlation between these two changes, we investigated  $\Delta$ (N)TCP and  $\Delta\gamma$  separately.  $\Delta$ (N)TCP was defined as the (N)TCP value when DCGS=2.0mm minus the (N)TCP value when DCGS was the other value.  $\Delta\gamma$  was defined as 100.0% minus the  $\gamma$  passing rate when the dose of DCGS=3.0mm, or 4.0mm, or 5.0mm compared that of DCGS=2.0mm. Because  $\gamma$  analysis was carried out with three different standards in this paper, the  $\Delta\gamma$  were divided into  $\Delta\gamma_1$ ,  $\Delta\gamma_2$  and  $\Delta\gamma_3$  corresponding to 1.0mm, 1.0%, 10.0%; 1.0mm, 2.0%, 10.0% and 1.0mm, 3.0%, 10.0%.

In order to simplify the following writing, we describe the corresponding relationship as follows.

"M" corresponding to  $\Delta$  (N)TCP = (N)TCP(DCGS=2.0mm) - (N)TCP(DCGS=3.0mm) and

$\Delta\gamma = 100.0\%$  -  $\gamma$  passing rate when DCGS=3.0mm compared DCGS=2.0mm.

"N" corresponding to  $\Delta$  (N)TCP = (N)TCP(DCGS=2.0mm) - (N)TCP(DCGS=4.0mm) and

$\Delta\gamma = 100.0\%$  -  $\gamma$  passing rate when DCGS=4.0mm compared DCGS=2.0mm.

"L" corresponding to  $\Delta$  (N)TCP = (N)TCP(DCGS=2.0mm) - (N)TCP(DCGS=5.0mm) and

$\Delta\gamma = 100.0\%$  -  $\gamma$  passing rate when DCGS=5.0mm compared DCGS=2.0mm.

The  $\Delta$  (N)TCP and  $\Delta\gamma$  were shown in Table 3, Table 4 and Table 5. As shown in the tables, when the calculated values of (N)TCP of the targets, the bladder and the rectum decreased with DCGS increasing, the  $\gamma$  passing rate also decreased when the standard was 1.0mm, 1.0%, 10.0%.

## Discussion And Conclusion

Compared with conformal radiotherapy, intensity-modulated radiotherapy can improve the conformal degree of the target area, reduce the dose of organs at risk, and reduce the acute and late toxicity of organs[28,29]. VMAT is a higher form of modulated radiation therapy, VMAT and IMRT have been compared in many studies[30,31]. The publications relating to planning[32], commissioning[33], QA [34] and clinical implementation[35] have been published, which made VMAT technology spread quickly around the world. VMAT technology is widely used for the CC radiotherapy. These studies on the application have shown that VMAT technology can be used for cervical cancer radiotherapy, and compared with High Dose Rate brachytherapy, VMAT plan achieves significant dose reduction of rectum, bladder and sigmoid, as well as superior homogeneous target coverage compared to brachytherapy plan[36-38]. Therefore, the CCs' VMAT plans were selected as the research object in this study. Gantry rotation speed and dose rate vary when a VMAT schedule is executed, which made the complexity of VMAT QA be more than that of IMRT[39]. As the origins of QA failure could be uneasy to confirm this failure caused by dose calculation from TPS, or dose delivery from linac, or detectors of phantom, or other aspects. Therefore, the source of the (N)TCP and  $\gamma$  passing rate was fixed on one factor DCGS.

It is an important basis for us to set up DCGS in the planning design to consider the efficiency of calculation under the precise of satisfying the accuracy of dose calculation. Many studies from radiation oncology departments recommend DCGS=2.0mm be for the clinical requirements[40,41]. This conclusion was the main reason why in this paper we chose DCGS=2.0mm as the research basis. Secondly, the low computational efficiency of DCGS=1.0mm makes it difficult in clinical practice, when was DCGS=1.0mm, the Pinnacle TPS would spend about two 2.0 hours to calculate once a dose distribution for a patient.

Gamma analysis is a commonly used method to compare differences between two dose distributions, but the ability of gamma analysis to detect errors is closely related to the criteria set. Fig. 7 of the "**p-value analysis**" in this paper showed that when 1.0mm, 1.0% and 10.0% was used as the standard in the  $\gamma$  analysis, there was a statistical difference ( $p < 0.05$ ) between any two results of  $\gamma$  analysis when DCGS was 3.0mm, 4.0mm or 5.0mm vs 2.0mm, indicating that the Gamma analysis was sensitive to changes of DCGS. However, when 1.0mm, 3.0% and 10.0% was used as the standard in  $\gamma$  analysis, there was mostly no significant difference ( $p > 0.05$ ) between any two results of  $\gamma$  analysis when DCGS was 3.0mm, 4.0mm or 5.0mm vs 2.0mm, and at this time the Gamma analysis was not sensitive to changes of DCGS. Many studies' results all reflected the similar conclusion of  $\gamma$ -standard and  $\gamma$  analysis's sensitivity[42,43]. The difference was that these studies had set change of the standard in two dimensions (distance and dose) at the same time, for example, change the  $\gamma_{3.0\% \square 3.0\text{mm}}$  to  $\gamma_{2.0\% \square 2.0\text{mm}}$ . When the dose standard of  $\gamma$  analysis was relaxed from 1.0% to 3.0%, the "dose points" of  $1.0\% < \text{dose error} < 3.0\%$  that failed with the standard of 1.0mm, 1.0% and 10.0% were allowed to pass, so the ability of  $\gamma$  analysis to detect dose error  $\in [1.0\%, 3.0\%]$  was losing. At the same time, we could also get from the results that the majority of the dose "calculated value" changes as DCGS from 2.0mm to 5.0mm were  $< 3.0\%$ .

However, the situation was different when the (N)TCP biological mathematical model was used to detect these dose changes, and theoretically any DS caused by DCGS could be represented in the value of (N) TCP as long as the value of (N) TCP was accurate enough. So, when we changed DCGS we got the trend of (N) TCP and  $\Delta$  (N) TCP, even though  $\Delta$  (N) TCP was not a big value. In the study,  $\Delta$  NTCP of the Femurs was always 0.00 in Table 5. It was not because NTCP did not change, but because the value was omitted because of too small, which was caused by parameters' value of NTCP model.

The TCP and NTCP were expected to be obtained by studying the targets' and OARs' physical dose, because the two formers were of greater clinical significance. So this paper studied the relationship between  $\Delta$ (N)TCP and  $\Delta\gamma$ . With the DCGS becoming larger, the relatively-lower-dose in the normal tissues located around the target was more calculated into the target, so the overall dose of the target decreased and the TCP decreased. The focused irradiation mode of radiotherapy determines the general trend of dose decrease from the target area to the periphery, with the highest dose in the target. In this paper, we investigated the OARs, bladder, rectum, and femurs were the organs of adjacent to the targets, as the DCGS became larger, their relatively-high-dose was "deprived" by the targets, and the dose "deprived" by them from their surrounding was relatively-high-dose, so the DCGS became larger, their overall doses were falling, and their NTCPs were falling.

The 3DVH- $\gamma$  analysis and bio-mathematical model can be used to analyze the effect of DCGS on the planned dose, and the former's detection ability has a lot to do with the designed standard, and the latter's capability is related to the parameters and calculated accuracy of the latter.

## Abbreviations

DCGS	dose calculation grid size;
PD	planned dose
DVH	dose-volume histogram;
RDS	reference data set
MDS	measurement data set
TCP	tumor control probability
NTCP	normal tissue complication probability
TPS	treatment planning system
OAR	organ-at-risk
CC	cervical cancer

DD dose distribution

IMRT intensity modulated radiation therapy

VMRT volumetric modulated arc therapy

PTV planning target volume

PGTV planning gross tumor volume

## **Declarations**

### **Acknowledgements**

Not applicable.

### **Authors' contributions**

HB conducted all digital analyses and performed the statistical analysis. HB and XRW made substantial contributions to the conception and design of the work. HB, SJZ and XHL were major contributors in drafting and writing the manuscript. FHC, JWY, SJZ were responsible for radiation treatment planning. The author(s) read and approved the final manuscript.

### **Funding**

The authors have received the financial support from the planned project of science and technology department of yunnan province of China. Item number is 2017FE468(-221).

### **Availability of data and materials**

The datasets generated and/or analysed during the current study are not publicly available due to the General Data Protection Regulation (GDPR) but are available from the corresponding author on reasonable request.

### **Ethics approval and consent to participate**

Not applicable.

### **Consent for publication**

The authors agreed to publish this paper in Radiation Oncology

### **Competing interests**

The authors declare that they have no competing interests.

## Author details

1 Department of Radiation Oncology, The Third Affiliated Hospital of Kunming Medical University, Yunnan Tumor Hospital, Kunming, Yunnan, China.

Full postal address: Department of Radiation Oncology, Tumor Hospital of Yunnan Province, No.519 Kunzhou

Road, Xishan District, Kunming, China

## References

- [1] Park, JM; Park, SY; Kim, JI; et al. The influence of the dose calculation resolution of VMAT plans on the calculated dose for eye lens and optic pathway [J]. *Australas Phys Eng Sci Med*, 2017, 40(1):209-217
- [2] SS, Gou; RW, Jiang, QE, Ding, et al. Effects of mesh accuracy on radiotherapy plan for different cancers[J]. *Chin J Cancer Prev Treat*, 2017, 24(20): 1465-1468
- [3] Lam D; Zhang X; Li H; et al. Predicting gamma passing rates for portal dosimetry-based IMRT QA using machine learning[J]. *Med Phys*, 2019, 46(10) :4666-4675
- [4] Han, C; Yu, W; Zheng, X; et al. Composite QA for intensity-modulated radiation therapy using individual volume-based 3D gamma indices[J]. *J Radiat Res*, 2018, 59(5) :669-676
- [5] Low, DA ; Harms, WB ; Mutic, S ;et al. A technique for the quantitative evaluation of dose distributions[J]. *Med Phys*, 1998, 25(5) :656-61
- [6] Ezzell, GA ; Burmeister, JW ; Dogan, N ; et al. IMRT commissioning: multiple institution planning and dosimetry comparisons, a report from AAPM Task Group 119[J]. *Med Phys*, 2009, 36(11) :5359-73
- [7] Shiba, E; Saito, A; Furumi, M; et al. Predictive gamma passing rate by dose uncertainty potential accumulation model[J]. *Med Phys*, 2019, 46(2) :999-1005
- [8] Zhang, D; Wang, B ; Zhang, G; et al. Comparison of 3D and 2D gamma passing rate criteria for detection sensitivity to IMRT delivery errors[J]. *J Appl Clin Med Phys*, 2018, 19(4) :230-238
- [9] Hussein, M; Rowshanfarzad, P; Ebert, MA; et al. A comparison of the gamma index analysis in various commercial IMRT/VMAT QA systems[J]. *Radiother Oncol*,2013, 109(3) :370-6
- [10] Heilemann, G ; Poppe, B ; Laub, W. On the sensitivity of common gamma-index evaluation methods to MLC misalignments in Rapidarc quality assurance[J]. *Med Phys*, 2013, 40(3) :031702-1-13
- [11] Zhen, H; Hrycushko, B; Lee, H; et al. Dosimetric comparison of Acuros XB with collapsed cone convolution/superposition and anisotropic analytic algorithm for stereotactic ablative radiotherapy of thoracic spinal metastases[J]. *J Appl Clin Med Phys*, 2015, 16(4) :181-192

- [12] De Deene, Y. Gel dosimetry for the dose verification of intensity modulated radiotherapy treatments[J]. *Z Med Phys*, 2002, 12(2) :77-88
- [13] Ibbott, GS ; Maryanski, MJ ; Eastman, P ; et al. Three-dimensional visualization and measurement of conformal dose distributions using magnetic resonance imaging of BANG polymer gel dosimeters[J]. *Int J Radiat Oncol Biol Phys*, 1997,38(5) :1097-103
- [14] Jursinic, PA ; Sharma, R ; Reuter, J. MapCHECK used for rotational IMRT measurements: Step-and-shoot, Tomotherapy, RapidArc[J]. *Med Phys*, 2010,37(6Part1) :2837-2846
- [15] Varasteh Anvar M ; Attili, A ; Ciocca, M ; et al. Quality assurance of carbon ion and proton beams: A feasibility study for using the 2D MatriXX detector[J]. *Phys Med*. 2016 Jun ;32(6) :831-7
- [16] Bedford, JL; Fast, MF; Nill, S; et al. Effect of MLC tracking latency on conformal volumetric modulated arc therapy (VMAT) plans in 4D stereotactic lung treatment[J]. *Radiother Oncol*, 2015, 117(3) :491-495
- [17] Morrison, CT ; Symons, KL ; Woodings, SJ; et al. Verification of junction dose between VMAT arcs of total body irradiation using a Sun Nuclear ArcCHECK phantom[J]. *J Appl Clin Med Phys*, 2017 , 18(6) :177-182
- [18] Yang, B; Geng, H; Ding, Y; et al. Development of a novel methodology for QA of respiratory-gated and VMAT beam delivery using Octavius 4D phantom[J]. *Med Dosim*, 2019, 44(1) :83-90
- [19] Alharthi, T ; Pogson, EM ; Arumugam, S ; et al. Pre-treatment verification of lung SBRT VMAT plans with delivery errors: Toward a better understanding of the gamma index analysis[J]. *Phys Med*, 2018,49(5) :119-128
- [20] Kim, JI ; Park, SY ; Kim, HJ ; et al. The sensitivity of gamma-index method to the positioning errors of high-definition MLC in patient-specific VMAT QA for SBRT[J]. *Radiat Oncol*, 2014, 28 (9) :167-176
- [21] 3DVH Reference Guide – Complete 3D Patient Dose Analysis[M]. 2018,93-93
- [22] Chow, JL; Jiang, R. Dose-volume and radiobiological dependence on the calculation grid size in prostate VMAT planning [J]. *Med Dosim*, 2018, 43(4):383-389
- [23] Gulliford, SL; Partridge, M; Sydes, MR; et al. Parameters for the Lyman Kutcher Burman (LKB) model of Normal Tissue Complication Probability (NTCP) for specific rectal complications observed in clinical practise [J]. *Radiother Oncol*, 2012, 102(3):347-351
- [24] Luxton, G; Keall, PJ; King, CR. A new formula for normal tissue complication probability (NTCP) as a function of equivalent uniform dose (EUD) [J]. *Phys Med Biol*, 2008, 53(1):23- 36
- [25] Fogliata, A; Thompson, S; Stravato, A; et al. On the gEUD biological optimization objective for organs at risk in Photon Optimizer of Eclipse treatment planning system [J]. *J Appl Clin Med Phys*, 2018,

- [26]Aras, S ; İkizceli, T ; Aktan, M. Dosimetric Comparison of Three-Dimensional Conformal Radiotherapy (3D-CRT) and Intensity Modulated Radiotherapy Techniques (IMRT) with Radiotherapy Dose Simulations for Left-Sided Mastectomy Patients[J]. Eur J Breast Health, 2019, 15(2) :85-89
- [27]Johansen, S ; Cozzi, L ; Olsen, DR. A planning comparison of dose patterns in organs at risk and predicted risk for radiation induced malignancy in the contralateral breast following radiation therapy of primary breast using conventional, IMRT and volumetric modulated arc treatment techniques[J]. Acta Oncol, 2009, 48(4) :495-503
- [28]Cho, KH; Kim, JY ; Lee, SH; et al. Simultaneous integrated boost intensity-modulated radiotherapy in patients with high-grade gliomas[J]. Int J Radiat Oncol Biol Phys, 2010, 78(2) :390-7
- [29]Daly-Schveitzer, N ; Juliéron, M ; Tao, YG ; et al. Intensity-modulated radiation therapy (IMRT): toward a new standard for radiation therapy of head and neck cancer?[J]. Eur Ann Otorhinolaryngol Head Neck Dis, 2011 ,128(5) :241-7
- [30] Ouyang, Z ; Liu Shen, Z ; Murray, E ; et al. Evaluation of auto-planning in IMRT and VMAT for head and neck cancer[J]. J Appl Clin Med Phys, 2019, 20(7) :39-47
- [31] Wiehle, R ; Knippen, S ; Grosu, AL ; et al. VMAT and step-and-shoot IMRT in head and neck cancer: a comparative plan analysis[J]. Strahlenther Onkol, 2011, 187(12) :820-5
- [32] Ezzell, GA ; Galvin, JM ; Low, D ;et al. Guidance document on delivery, treatment planning, and clinical implementation of IMRT: report of the IMRT Subcommittee of the AAPM Radiation Therapy Committee[J]. Med Phys, 2003, 30(8) :2089-115
- [33] Ezzell, GA ; Burmeister, JW ; Dogan, N ;et al. IMRT commissioning: multiple institution planning and dosimetry comparisons, a report from AAPM Task Group 119[J]. Med Phys, 2009, 36(11) :5359-73
- [34]Basran, PS ; Woo, MK; et al. An analysis of tolerance levels in IMRT quality assurance procedures[J]. Med Phys, 2008, 35(6) :2300-7
- [35]McNair, HA ; Adams, EJ ; Clark, CH ; et al. Implementation of IMRT in the radiotherapy department[J]. Br J Radiol, 2003,76(912) :850-6
- [36] Tinoco, M ; Waga, E ; Tran, K ; et al. RapidPlan development of VMAT plans for cervical cancer patients in low- and middle-income countries[J]. Med Dosim, 2020, 45(2):172-178
- [37] Wali, L ; Helal, A ; Darwesh, R ; et al. A dosimetric comparison of Volumetric Modulated Arc Therapy (VMAT) and High Dose Rate (HDR) brachytherapy in localized cervical cancer radiotherapy[J]. J Xray Sci Technol, 2019, 27(3) :473-483

- [38] Wang, Y ; Chen, L ; Zhu, F ; et al. A study of minimum segment width parameter on VMAT plan quality, delivery accuracy, and efficiency for cervical cancer using Monaco TPS[J]. J Appl Clin Med Phys, 2018 Sep , 19(5) :609-615
- [39] Sanghangthum, T ; Suriyapee, S ; Srisatit, S ; et al. Statistical process control analysis for patient-specific IMRT and VMAT QA[J]. J Radiat Res, 2013,54(3) :546-52
- [40] Park, JY ; Kim, S ; Park, HJ ;et al. Optimal set of grid size and angular increment for practical dose calculation using the dynamic conformal arc technique: a systematic evaluation of the dosimetric effects in lung stereotactic body radiation therapy[J]. Radiat Oncol, 2014, 9(4 ) :5-12
- [41] Gros, S ; Descovich, M ; Barani, I ;et al. SU-E-T-446: Effect of Dose Calculation Grid Size Variability on the Specification of Spinal Cord Dose Tolerance for Spinal Stereotactic Body Radiation Therapy[J]. Med Phys, 2012 Jun ;39(6Part17) :3807
- [42] Bresciani, S ; Di Dia, A ; Maggio, A ;et al. Tomotherapy treatment plan quality assurance: the impact of applied criteria on passing rate in gamma index method[J]. Med Phys, 2013, 40(12) :121711-20
- [43] Templeton, AK ; Chu, JC ; Turian, JV. The sensitivity of ArcCHECK-based gamma analysis to manufactured errors in helical tomotherapy radiation delivery[J]. J Appl Clin Med Phys, 2015, 16(1) :4814-22

## Tables

**Table 1** Dose-volume criteria used in the cervix cancer VMAT plans

Volume of interest	Dose-volume criteria (cGy)
PGTV	MinD=95%PD, $V_{PD} \geq 95\%$ , MaxD=107%PD
PTV	MinD=95%PD, $V_{PD} \geq 95\%$ , MaxD=107%PD
Rectum	$V_{40} < 60\%$ , $D_{33\%} < 45\text{Gy}$
Bladder	$V_{40} < 40\%$ , $D_{33\%} < 45\text{Gy}$
L-Femur	$V_{45} < 5\%$ , $V_{30} < 30\%$
R-Femur	$V_{45} < 5\%$ , $V_{30} < 30\%$
Intestine	$V_{30} < 30\%$
Cord	MaxD=45Gy

Note: PD is the prescribed dose

**Table 2** The group and name of  $\gamma$  analysis results

DCGS	$\gamma$ -Cri	1.0mm, 1.0%, 10.0%	1.0mm, 2.0%, 10.0%	1.0mm, 3.0%, 10.0%
3.0mm vs 2.0mm	Aa		Ab	Ac
4.0mm vs 2.0mm	Ba		Bb	Bc
5.0mm vs 2.0mm	Ca		Cb	Cc

Table 3. Display of  $\Delta$ TCP and  $\Delta\gamma$

<i>Name</i>	<i>PGTV</i>				<i>PTV</i>			
	$\Delta$ TCP	$\Delta\gamma1$	$\Delta\gamma2$	$\Delta\gamma3$	$\Delta$ TCP	$\Delta\gamma1$	$\Delta\gamma2$	$\Delta\gamma3$
M	0.40	0.20	0.00	0.00	0.40	0.86	0.27	0.00
N	0.90	1.63	0.20	0.00	0.70	1.47	0.61	0.00
L	1.40	10.61	0.71	0.00	1.10	6.75	1.66	0.48

Table 4. Display of  $\Delta$ NTCP and  $\Delta\gamma$  for the bladder and the rectum

<i>Name</i>	<i>Bladder</i>				<i>Rectum</i>			
	$\Delta$ NTCP	$\Delta\gamma1$	$\Delta\gamma2$	$\Delta\gamma3$	$\Delta$ NTCP	$\Delta\gamma1$	$\Delta\gamma2$	$\Delta\gamma3$
M	0.20	0.50	0.12	0.00	0.30	0.08	0.16	0.03
N	0.40	1.54	0.69	0.37	0.60	2.15	0.40	0.40
L	0.50	4.58	1.22	0.33	0.90	2.99	1.42	0.00

Table 5. Display of  $\Delta$ NTCP and  $\Delta\gamma$  for the femurs

<i>Name</i>	<i>L-Femur</i>				<i>R-Femur</i>			
	$\Delta$ NTCP	$\Delta\gamma1$	$\Delta\gamma2$	$\Delta\gamma3$	$\Delta$ NTCP	$\Delta\gamma1$	$\Delta\gamma2$	$\Delta\gamma3$
M	0.00	0.02	0.00	0.00	0.00	0.17	0.00	0.00
N	0.00	1.07	0.19	0.01	0.00	0.75	0.02	0.00
L	0.00	2.93	0.60	0.08	0.00	1.70	0.33	0.00

## Figures

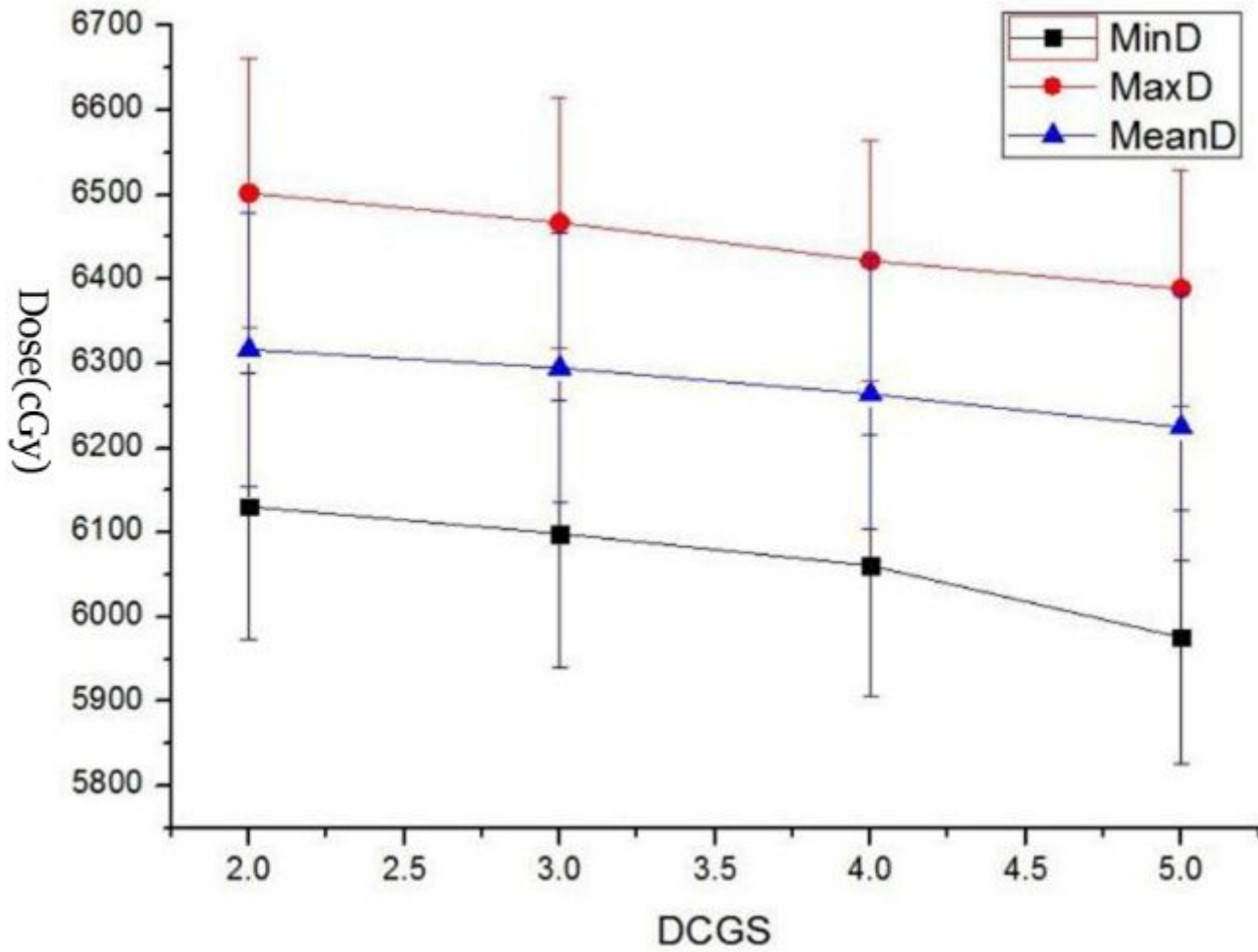


Figure 1

Display of MinD, MaxD and MeanD of PGTV change caused by DCGS

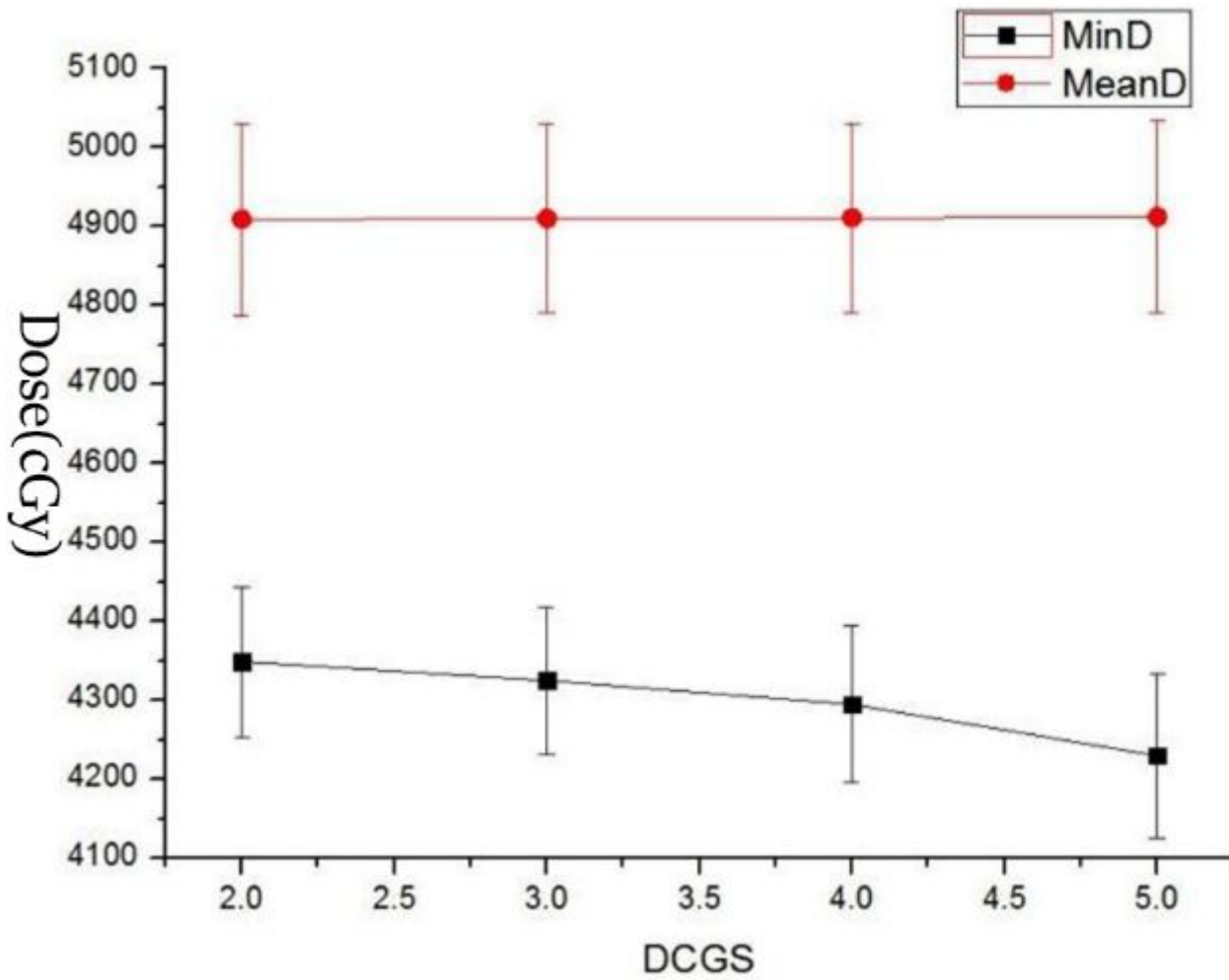


Figure 2

Display of MinD and MeanD of PTV change casused by DCGS

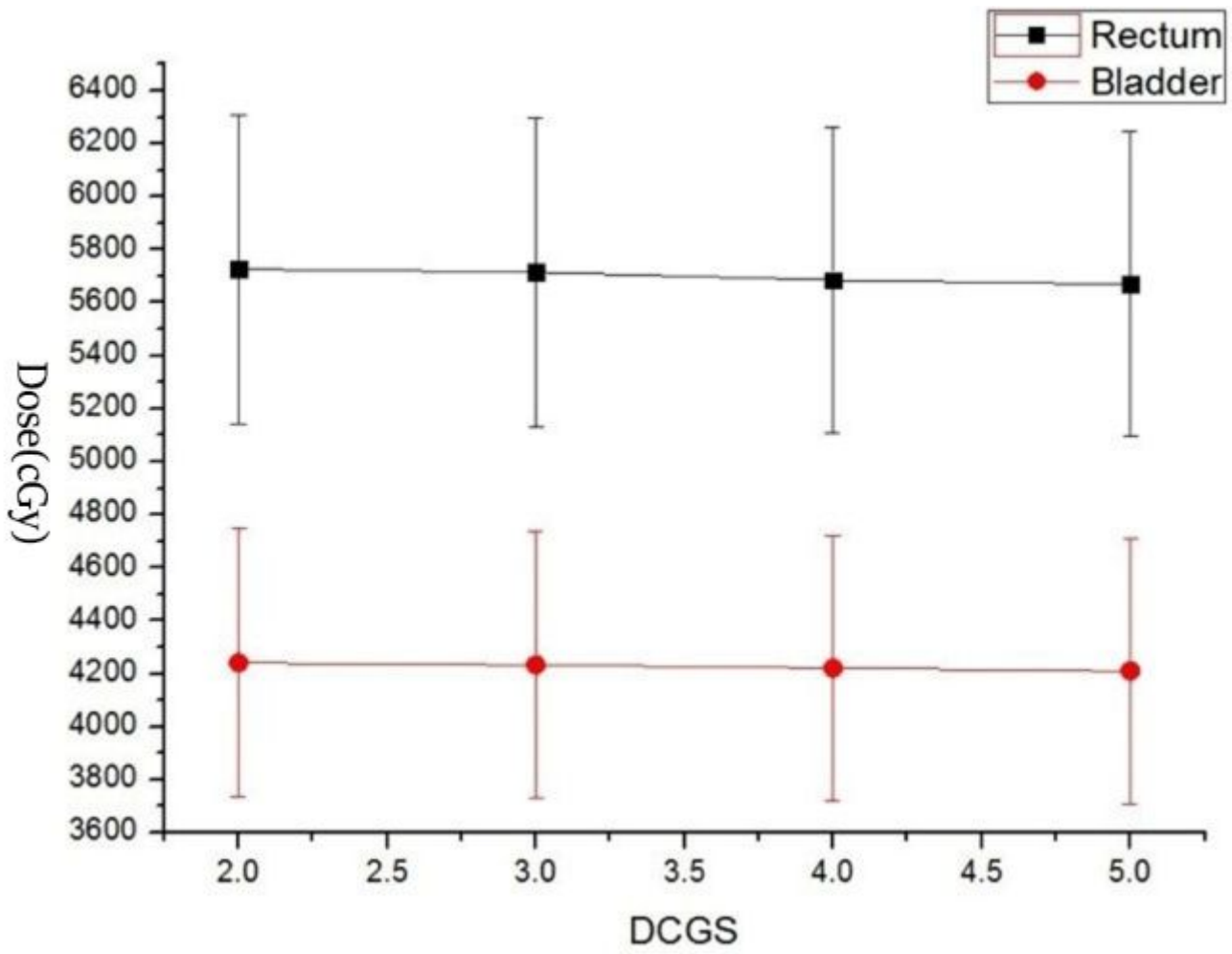


Figure 3

Display of MeanDs of Rectum and Bladder change casused by DCGS

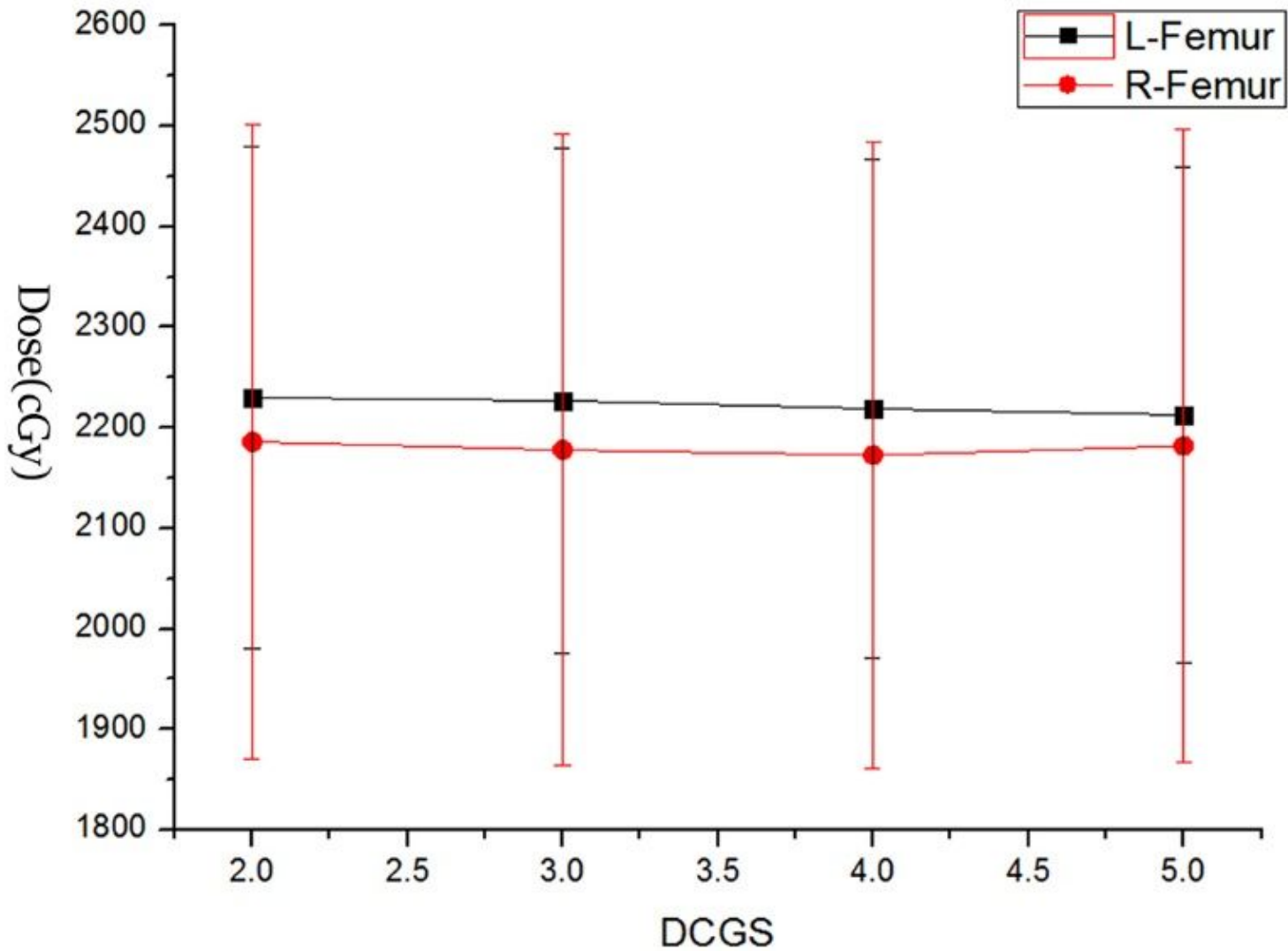


Figure 4

Display of MeanDs of R-Femur and L-Femur change casused by DCGS

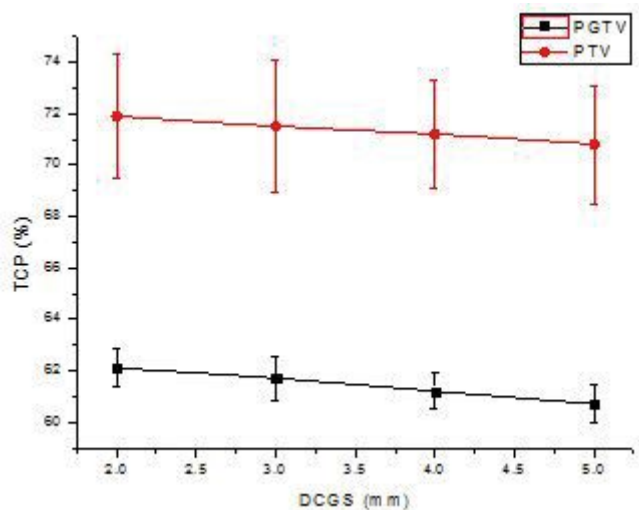


Figure 5

## Display of TCP change casused by DCGS

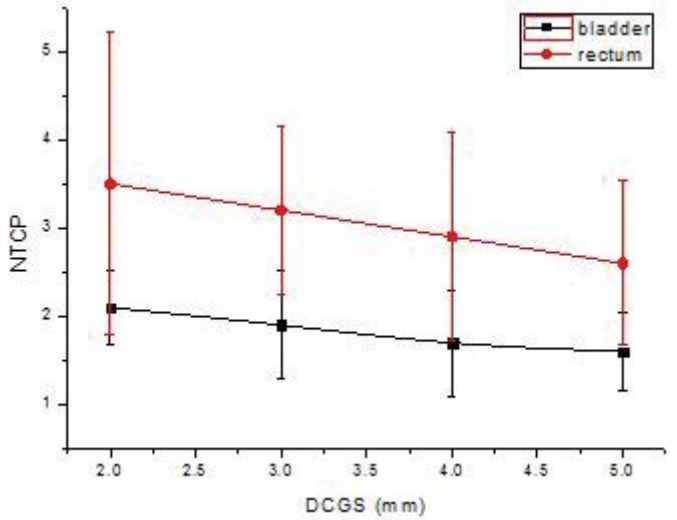


Figure 6

## Display of NTCP change casused by DCGS

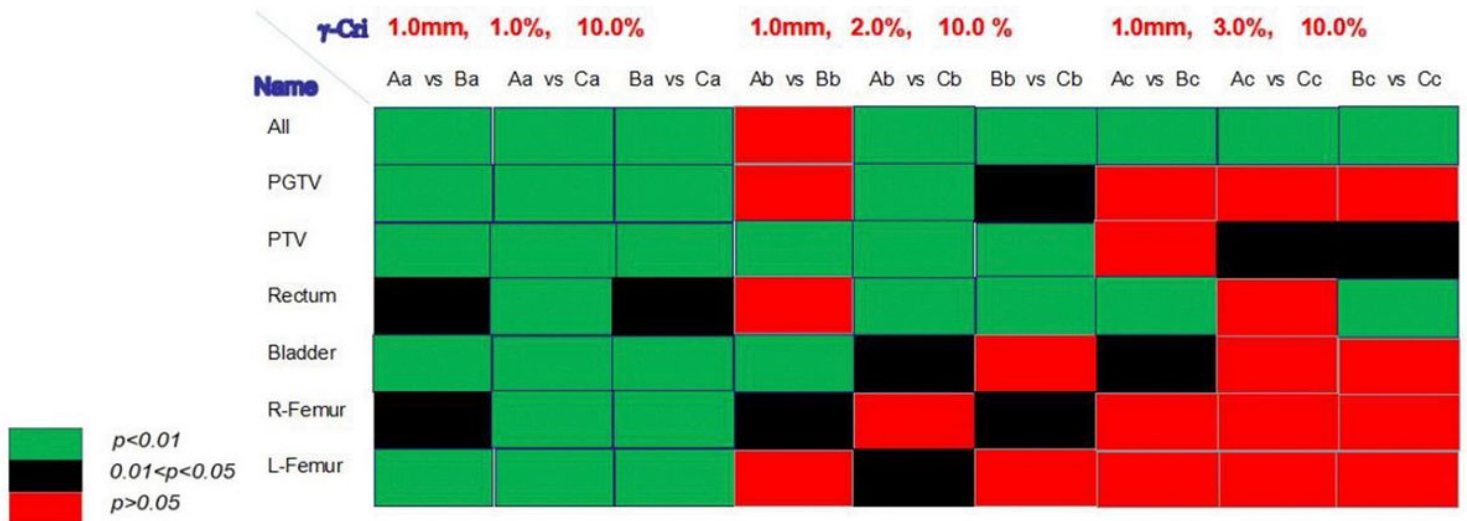


Figure 7

The map of every structure's paired t test under varied  $\gamma$  analysis standard.

## Supplementary Files

This is a list of supplementary files associated with this preprint. Click to download.

- [Equations.docx](#)